4 CORNEAL ONLAYS FROM CROSSLINKED ARTIFICIAL EXTRACELLULAR MATRIX PROTEINS

4.1 Abstract

An artificial protein designed to mimic key features of the extracellular matrix is proposed for use in corneal onlays. The protein contains an elastin-like repeating sequence to confer flexibility and a fibronectin-derived cell binding domain containing the peptide RGD (Arg-Gly-Asp) to promote adhesion of corneal epithelial cells. The protein was crosslinked through its lysine side chains with bis(sulfosuccinimidyl) suberate (BS3). The resulting onlay lenses were highly extensible (>350% strain) and had a Young's modulus of 0.17 ± 0.02 MPa. Implantation of the crosslinked lenses in rabbits (n=12) for one week indicated that the onlays were well-tolerated in the cornea. The onlays had fully re-epithelialized within 4-7 days of implantation, compared to 2-4 days for native corneal stroma. The cell morphology on the onlay implant was typical of regenerating epithelium, and only minimal inflammation was observed.

Manuscript prepared for submission by Paul J. Nowatzki[1], Daniel M. Schwartz[2], Marsha Cheung[2], Shiao Chang[3], Robert H. Grubbs[1], and David A. Tirrell[1]

(1) Division of Chemistry and Chemical Engineering, California Institute of Technology
(2) Department of Ophthalmology, University of California, San Francisco
(3) Calhoun Vision, Pasadena, CA

Portions of the Experimental and Results sections appear in U.S. Patent Application No. 11/040,130 (filed 1/23/2005). "Engineered Proteins and Methods of Making and Using." inventors David A. Tirrell, Daniel M. Schwartz, Paul J. Nowatzki, Robert H. Grubbs.

4.2 Introduction

Surgical procedures to correct refractive error, especially laser in situ keratomileusis (LASIK) and photorefractive keratectomy (PRK), have proven effective in the correction of myopia, astigmatism, and low to moderate hyperopia. However, these procedures have limited efficacy in the correction of high hyperopia and very high myopia.[1] Furthermore, the lack of reversibility of these procedures is a major drawback, because the refractive power of the cornea may change over time. In this work we describe the implantation of corneal onlays made from an artificial protein, with the ultimate goal of achieving a reversible but stable means for surgical refractive correction.

Corneal implants have recently attracted attention as reversible alternatives to ablative surgeries.[2] An implant would be designed based on its shape and index of refraction to change the refractive properties of the cornea in a prescribed way. The implant can be placed inside a flap cut into the corneal stroma (keratoplasty), called a *corneal inlay*, or at the anterior surface of the corneal stroma, just under the corneal epithelium (epikeratoplasty), called a *corneal onlay* (see Figure 4.1). The epithelium can be scraped off, or debrided, allowing the epithelium to grow back over the surface of the onlay. Alternatively, an epithelial flap can be peeled back and replaced on top of the onlay, reducing healing time, as is done in the ablative LASEK (laser epithelial keratomileusis) technique.[3]

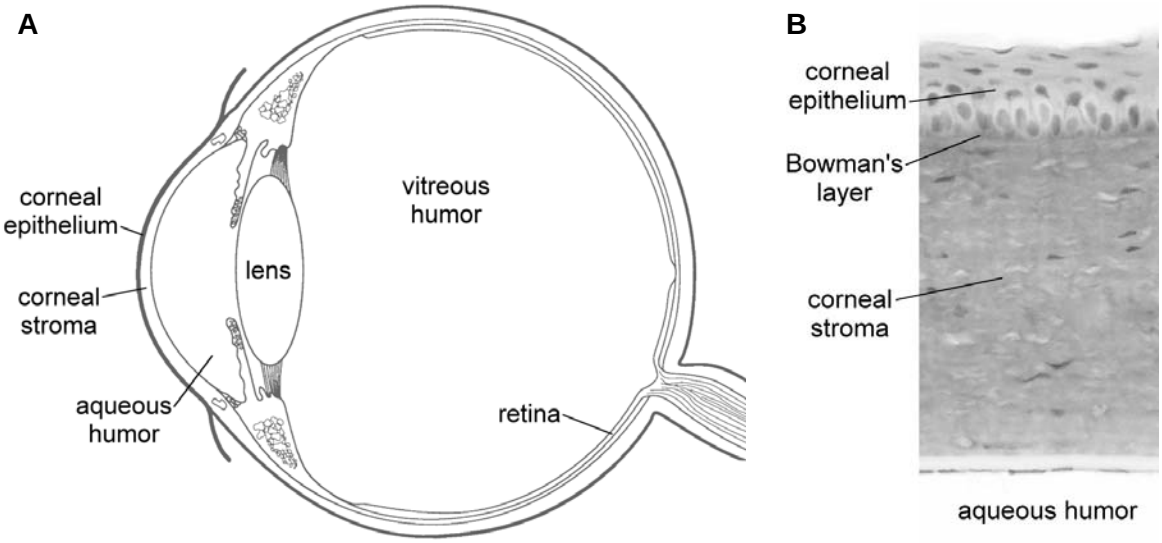

Figure 4.1 (A) Structure of the eye. (B) Histological cross-section of the cornea. A corneal onlay resides between the cellular corneal epithelium and collagenous stroma; an inlay is placed inside the stroma. The human cornea is 550 μm thick.

(B adapted from http://www.webmed.unibo.it/didattica/pezzetti/Connettivi/cornea20he.jpg)

The implantation of corneal onlays is particularly appealing because of its surgical simplicity, which, unlike LASIK or placing a corneal inlay, does not require use of a microkeratome to cut a corneal flap. Obviating this incision may prevent certain surgical complications of LASIK, which include corneal flap abnormalities,[4,5] epithelial ingrowth,[5] night vision disturbances,[6] and microbial keratitis.[7] The forward positioning of an onlay in the cornea is also preferable both optically and in minimizing its disruption to nutrient flow.[2] Because an onlay is not held in place by a corneal flap, there must be a means of adhering an onlay to the sub-epithelial layer (Bowman's layer) of the cornea.

Materials of both biologic and synthetic origins have been tested as corneal onlays. Human corneal tissue grafts resulted in abnormalities in epithelial cell physiology and extracellular matrix.[8-10] Because collagen is the primary component of corneal stroma, onlay lenses were made from collagen type IV, but these degraded over time.[11] This lack of stability due to proteolysis was seen in other collagen-based and collagen-hybrid lenses.[2] A consistent problem for synthetic corneal implants such as those made from poly(ethylene terephthalate), poly(methyl methacrylate), or polytetrafluoroethylene, on the other hand, is their inability to adhere an epithelium.[12,13] Synthetic materials designed for use as onlays that have been reported to support growth of epithelial cells include plasma-treated polyvinylalcohol copolymer hydrogels[14] and perfluoropolyethers, which were more effective when coated with collagen I.[2,15]

Based on these studies, the ideal properties of an effective corneal onlay material can be identified.[2,16] First, the material needs to be optically clear, dimensionally stable, and surgically handleable. A key requirement is its ability to adhere and permit migration and proliferation of epithelial cells. It must also be biocompatible over the long term, integrate closely with the surrounding tissue, not induce abnormal epithelial cell physiology, and be stable to proteases in the cornea. Ideally, its mechanical properties will be compatible with surrounding tissue and resistant to environmental stresses placed on the eye.

Biomimetic artificial proteins represent a new materials approach for corneal onlays. Genetic engineering has enabled the synthesis of proteins with

precisely controlled sequences and architectures.[17,18] These proteins should prove especially useful as biomaterials for several reasons. Their innate biocompatibility allows close interaction with surrounding tissue, potentially circumventing the foreign body reaction, which results in a fibrous capsule being formed around most synthetic polymer implants.[19] In particular, artificial proteins can include active peptide domains from natural proteins that promote cell adhesion[20] or direct cell differentiation.[21] Hybrid proteins containing modular combinations of structural, bioactive, and designed peptide sequences have been constructed,[18,22,23] with the idea of effecting multiple functionalities in a single material.

The work described here adapts an artificial protein, originally designed as a cell-adhesive material for use in vascular grafts, whose sequence is based on two naturally occurring extracellular matrix proteins, fibronectin and elastin. The amino acid sequence of the protein is shown in Figure 4.2. A 17-amino acid sequence taken from the tenth type III module of fibronectin including the RGD (Arg-Gly-Asp) sequence serves to support the adhesion and growth of an overlying epithelial cell layer. RGD is well-known to mediate adhesion through integrin cell-surface receptors to many cell types, thereby influencing morphology, migration, growth, and differentiation.[24] The RGD cell-binding domains are alternated with long sequences of elastin-like polypentapeptides that impart flexibility and resiliency. Elastin-like peptides of this type have been shown to be broadly biocompatible[25] and resistant to degradation,[26] and the highly dynamic, mobile structure of elastin[27] and elastin-like peptides[28] is

expected to facilitate diffusion through elastin-based matrices. Lysines are periodically spaced through the protein and serve as sites for crosslinking into stable matrices. This *artificial extracellular matrix protein* has been shown to attach endothelial cells specifically through the RGD cell binding domain,[23] and chemical crosslinking of similar materials resulted in transparent hydrogels with elastic moduli of 0.2 MPa.[29]

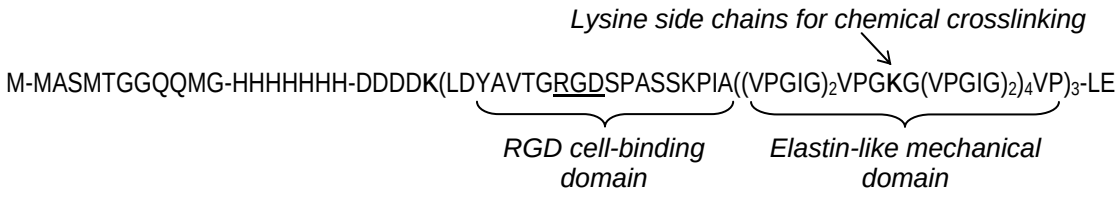

Figure 4.2 Amino acid sequence of the artificial extracellular matrix protein aE-RGD. The functions of key peptide elements are indicated.

It was hypothesized that this artificial extracellular matrix protein could be successful in corneal onlays because of its transparency, flexibility, resistance to degradation, permeability, and ability to adhere cells. Here, the artificial extracellular matrix protein was crosslinked into lens-shaped onlays, which were implanted into rabbit corneas using a corneal pocket model[30] and evaluated over the one week required for epithelialization. The results are sufficiently encouraging to merit longer-term implantation studies.

4.3 Experimental

4.3.1 Protein expression.

Protein aE-RGD, Figure 4.2, was cloned into *E. coli* by Liu et al.[23] The corresponding gene is under control of a T7 bacteriophage promoter: plasmid pET28RW-(RGD-EL4)$_3$.10a, expression host strain BL21 (DE3)pLysS. Its molecular weight is 34.8 kDa. The sequence contains three repeats of cell binding and elastin-like cassettes, with an N-terminal T7 tag for antibody identification, a 7-His tag for alternative purification, and an enterokinase cleavage site which can be used to remove the N-terminal portion.

Protein expression was performed as previously reported,[23] using standard methods. Briefly, host cells were grown in a 10 L fermenter (New Brunswick Scientific BioFlo 3000) using Terrific Broth medium at pH 7.4. At an optical density of ~6, protein expression was induced with 1 mM isopropyl-1-β-D-thiogalactosidase (IPTG); cells were harvested 1.25-1.75 hours after induction by centrifugation at 4°C.

4.3.2 Protein purification.

Cells containing the expressed aE-RGD protein were resuspended in TEN buffer (10 mM Tris-HC1, pH 7.5, 1 mM EDTA, 100 mM NaCl) at a concentration of 0.5 g/mL and frozen at -20°C. The suspension was defrosted, lysing the cells, and shaken with 10 μg/mL of deoxyribonuclease I, 10 μg/mL of ribonuclease A, 5 mM magnesium chloride, and 1 mM phenylmethylsulfonyl fluoride to inhibit

proteolysis, at 37 °C for 3 h. The lower critical solution temperature (LCST) of aE-RGD at 35 °C,[23] where the protein separates from an aqueous solution as the temperature is raised,[31] allows the protein to be purified by temperature cycling. The pH of the cell lysate was adjusted to 9.0, to ensure protein solubility, and the solution was centrifuged below the LCST (~1 h, ≥28,000×g, 4°C). To the supernatant (containing the protein), 1 M NaCl was added, and centrifugation was repeated above the LCST (~1 h, ≥28,000×g, 37°C). The pellet was redispersed in water to a concentration of 50-100 mg/mL. The temperature cycling was repeated twice more to increase protein purity. The solution containing the aE-RGD protein was dialyzed at 4°C for 3 days, to remove salts and contaminants, and lyophilized. The purity and molecular weights of the protein were verified by SDS-PAGE gels and Western blot, using standard methods, and confirmed previous[23] amino acid analysis and matrix-assisted laser desorption ionization-mass spectrometry (MALDI-MS) observations. Typical 10 L fermentations using these procedures yielded ~300 grams wet cell mass and 1 to 2 grams pure aE-RGD.

4.3.3 Cross-linking aE-RGD to form corneal onlays.

Two-piece poly(methylmethacrylate) contact lens molds of 6 mm optic diameter and 7.5 mm radius (Ocular Technology Inc., Goleta, CA) were used for forming corneal onlays. The molds created onlay lenses ~135 μm thick. The crosslinking procedure was adapted from Di Zio et al.[29] All crosslinking steps were performed in a cold room at 4 °C, below the LCST of aE-RGD,[23] to ensure

transparency of the lenses. aE-RGD (20 mg) was dissolved in water (55 μL). Bis(sulfosuccinimidyl) suberate (BS3), a lysine-specific crosslinking molecule, was dissolved in water (2.3 mg in 20 μL). The two solutions were rapidly mixed (10 sec) in a microcentrifuge tube by pipet tip and were quickly spun (10 sec) on a tabletop centrifuge to remove bubbles introduced in mixing. Into each of five molds, 12 μL of the mixture was pipetted; the molds were stacked under a weight (300g) and crosslinking proceeded overnight at 4 °C. Lenses were removed from the molds at room temperature, rinsed in excess water, and stored in a sealed humidified container until use.

4.3.4 Mechanical testing.

Rectangular pieces of lenses (~2 × 5 × 0.115 mm) were tested in an Instron 5542 uniaxial tensile tester, modified to house the sample in phosphate buffered saline at 37 °C, using a strain rate of 10% of the original length per minute.[32]

4.3.5 Surgical implantation of lenses.

The technique to implant the onlays was adapted from Evans et al.[30] The rabbits used in the study (n = 12, adult albino) were anesthetized using inhaled 3% isoflurane and topical proparacaine. Throughout the surgery, the vital signs of the animals were carefully monitored, including the corneal reflex, heart rate, respiration, and oxygen saturation.

To hold the lenses in place on the surface of the cornea, a pocket was created surgically, as shown in Figure 4.3. The right eye of each animal was

irrigated with betadine solution, and a wire lid speculum was placed into the eye. A 3.0 mm trephine was used to create a partial thickness keratotomy, approximately 100-200 μm in depth in the central cornea. The 0.12 forceps and the 69 blade were used to remove the stromal lamella within the trephined area from the base of the keratotomy. This left a circular keratectomy of 3.0 mm in diameter. A sharp pocket blade was used to make a 3 mm wide circular intralamellar pocket at the base of the keratotomy extending circumferentially outward toward the corneal limbus.

Three groups of corneas were prepared. In group 1 (n = 3), the wounds were created but no implants were placed. In group 2 (n = 12), the same wounds were constructed, and then the 5.0 mm diameter corneal onlay implant was carefully placed on the corneal surface. The implant was tucked 360 degrees into the grooved pocket using a blunt cyclodialysis spatula. No sutures were placed in this group. In group 3 (n= 3), the same wound was constructed, the implants were placed in the pocket, and then 9-0 Nylon sutures were placed over the implant to keep it into place. After implantation, the eyes were irrigated with BSS solution. The rabbits were given an injection of Carprofen analgesic (5 mg/kg IM) postoperatively.

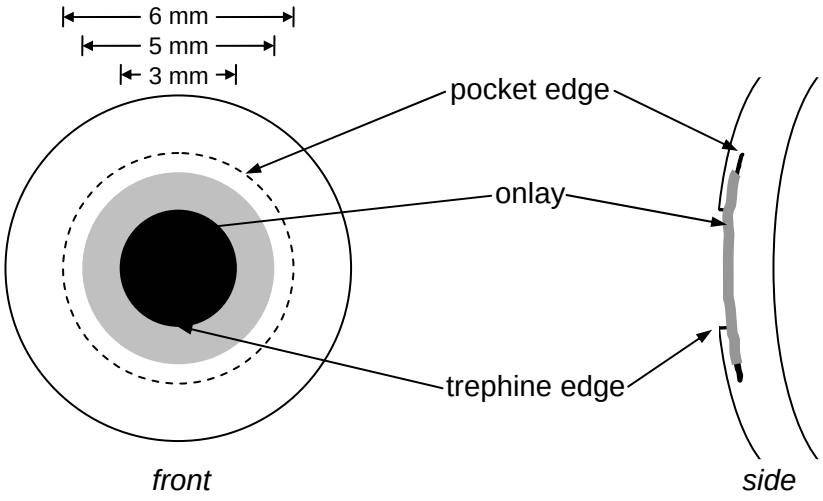

Figure 4.3 Schematic representation of the corneal pocket and implanted onlay lens.

4.3.6 Clinical evaluation.

Daily evaluation was performed for one week after implantation. The animals were closely followed for any signs of discomfort or wound infection. At any sign of discomfort, the animal was given one drop of topical 0.03% flurbiprofen and Carprofen 5 mg/kg IM q24 hours. The animals' weights were monitored. Slit lamp biomicroscopy was performed every 2-4 days following the initial procedure. Fluorescein staining with blue light was used to assess the speed and extent of epithelial cell growth on the onlays. Any signs of inflammation were noted.

4.3.7 Histology.

Rabbits were euthanized using standard guidelines for large animals, consisting of intramuscular ketamine 35-50 mg/kg and xylazine 5-10 mg/kg.

Each animal also received an intracardiac injection of sodium pentobarbital and underwent bilateral thoracotomy.

The eyes were fixed in glutaraldehyde solution and examined histologically at different time points. The slides were stained with hematoxylin-eosin (H&E), periodic acid-Schiff (PAS), Mason trichrome for collagen, and staining for mucopolysaccharides. Stained sections were mounted and viewed by light microscopy. The pattern of epithelial growth over the corneal implant was assessed histologically. The degree of inflammation both within the corneal stroma as well as within the implant was evaluated.

4.4 Results

4.4.1 Protein aE-RGD.

As shown in Figure 4.4A, the 35 kDa aE-RGD protein migrated as the predominant band on an SDS-PAGE Gel. Two minor bands are visible, indicating bacterial protein contaminants not fully removed during purification. T7-tag Western blotting, Figure 4.4B, confirmed the 35 kDa band as the aE-RGD protein.

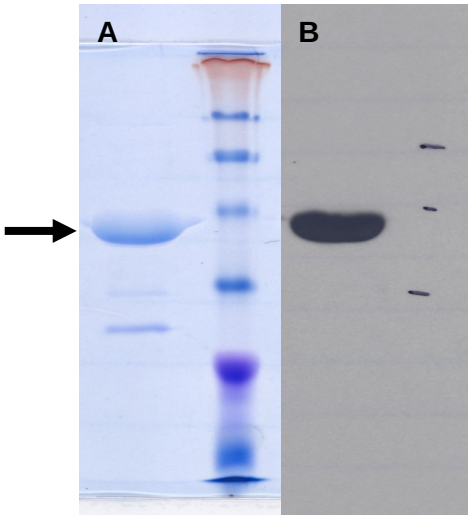

Figure 4.4 (A) SDS-PAGE and (B) Western blot analysis of aE-RGD. Minor impurity bands appear in the SDS-PAGE gel.

4.4.2 Mechanical characterization of lenses.

The crosslinked lenses remained transparent both during crosslinking at 4 °C, and when raised to 37 °C for mechanical testing. Because of the temperature-sensitive behavior of elastin-like protein films,[32,33] the onlays shrink from the 6.0 mm diameter × 0.135 mm thick mold dimensions to 5.0 mm diameter × 0.115 mm thick at 37 °C.

The tensile behavior of the lenses, shown in Figure 4.5, is characteristic of rubbery materials, consistent with previous tests of similarly designed artificial extracellular matrix proteins.[22,29,32] The elastic modulus, E, was measured to be 0.17 ± 0.02 MPa (n=3, from different batches), and each lens was extensible to at least 380% of its original length. Compared to BS3-crosslinked aECM proteins of similar design but different cell binding domain,[29] the lenses showed a similar elastic modulus but greater extensibility.

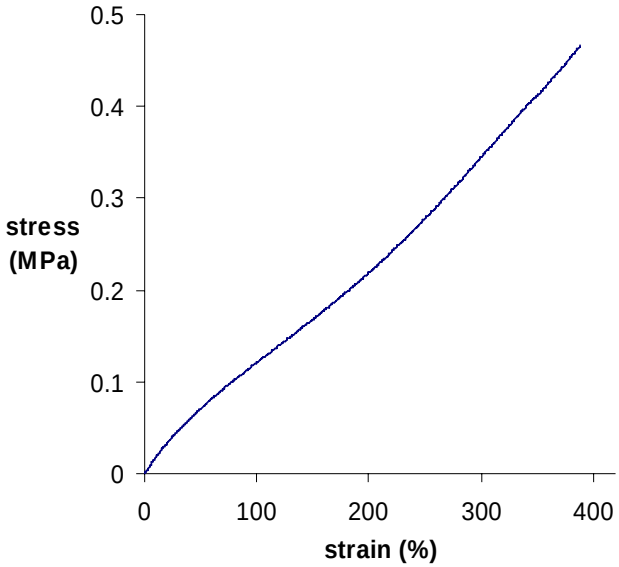

Figure 4.5 Representative uniaxial stress-strain behavior of a corneal onlay lens, tested at 37 °C in phosphate-buffered saline. E = 0.17 MPa.

The ability of the lenses to deform to high strains without failing is an advantage in their application as corneal onlays, which must withstand both surgical implantation and environmental forces once in place. The measured elastic modulus is similar to the 1 MPa suggested as an ideal compromise between the dual needs of compliance and wearer comfort, and sufficient stiffness for surgical handling.[2] If necessary, the modulus of the lenses could be decreased by reducing the crosslinker concentration. It could be increased by switching from a bi-functional to a tri-functional crosslinker (tris-succinimidyl aminotriacetate,[34] Pierce, Rockford, IL), or by re-engineering the protein sequence to contain more lysine side chains within the elastin-like domain. The range of elastic moduli observed in elastin-based artificial proteins, 0.03-35 MPa,[35] suggests that the basic design framework employed here could be adaptable to many materials needs.

4.4.3 Surgical implantation and observations.

The animals tolerated the procedure well and there were no surgical complications. The implants also tolerated the procedure well, as they were relatively easy to manipulate and durable during the surgery as long as they were well hydrated. Immediately postoperatively, the onlays remained intact and well positioned within the circular stromal pocket. There was a small difference in maintenance of the onlay in the proper position depending on whether sutures were placed or not, as three of the unsutured onlays fell out within the first 2-3 days of surgery. In the eyes where sutures were placed, the implants showed some surface wrinkling due to the tension that the sutures placed on the implant.

Compared to the controls, initial mild to moderate inflammation was observed in all the eyes with the implants, as shown by mild hyperemia of the bulbar conjunctiva and mild corneal stromal edema. There was no significant mucoid or purulent discharge noted in any of the animals.

4.4.4 Clinical evaluation.

Epithelialization, as visualized by fluorescein staining (Figure 4.6), in all cases initiated at the periphery of the exposed surface of the corneal onlays and progressed inward toward the center. The time required for full epithelialization varied somewhat between individual animals. The control eyes (sham surgery) showed commencement of epithelialization by day 1 and full epithelialization

within 2-4 days (not shown). All of the onlay animals (groups 2 and 3) showed epithelial cells on the periphery of the onlay by day 2 and full epithelialization within 4-7 days (Figure 4.6C). Results are summarized in Table 4.1.

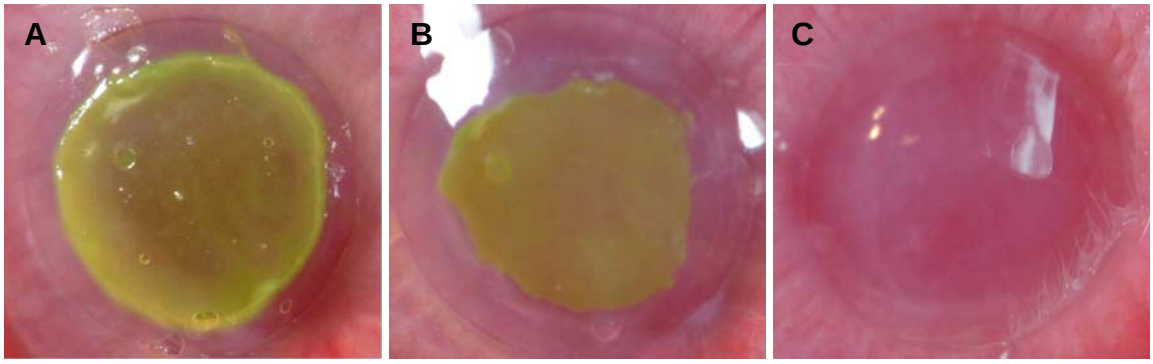

Figure 4.6 Fluorescein staining indicates the extent of re-epithelialization over the onlay surface. (A) Post-implantation, fluorescein stains the onlay up to the surgical defect edge. (B) At 2 days, re-epithelialization has begun to progress inward from the periphery. (C) At 7 days, the onlay is completely re-epithelialized.

Table 4.1 One week rabbit implantation study results

	Group 1 **Control: no onlay** n=5	Group 2 **Onlay** n=12	Group 3 **Onlay + sutures** n=3
Epithelial growth onto the debrided zone	Day 1	Day 2	Day 2
Full re-epithelialization	Day 2-4	Day 4-7	Day 4-7
Exam findings	Eyes quiet	Mild inflammation*	Mild inflammation**
Maintenance	-	9 of 12 remained in place at day 7	2 of 3 remained in place at day 7

* Mild signs of inflammation noted included mild corneal edema and ciliary flush.

** One eye was noted to have a large hypopyon and was sacrificed early.

4.4.5 Histology.

Epithelial cells had covered the entire implant at the time of examination one week after the surgery. The epithelium overlying the onlay appeared normal and consisted of 1-2 cell layers, typical for regenerating epithelium (Figure 4.7B). The interface between the corneal stroma and the implant was unremarkable, with some epithelial growth under the edges of the onlays (Figure 4.7A). The corneal stroma posterior to the onlay appeared normal. In a few cases, the corneal stroma and the corneal implant showed a moderate amount of inflammatory cells, including lymphocytes and neutrophils. In other cases, the stroma and implant appeared normal and free of inflammation.

At low magnification, Mason trichrome staining showed no staining of the novel onlay material compared to the natural cornea, indicating that no collagen was present in the onlay.

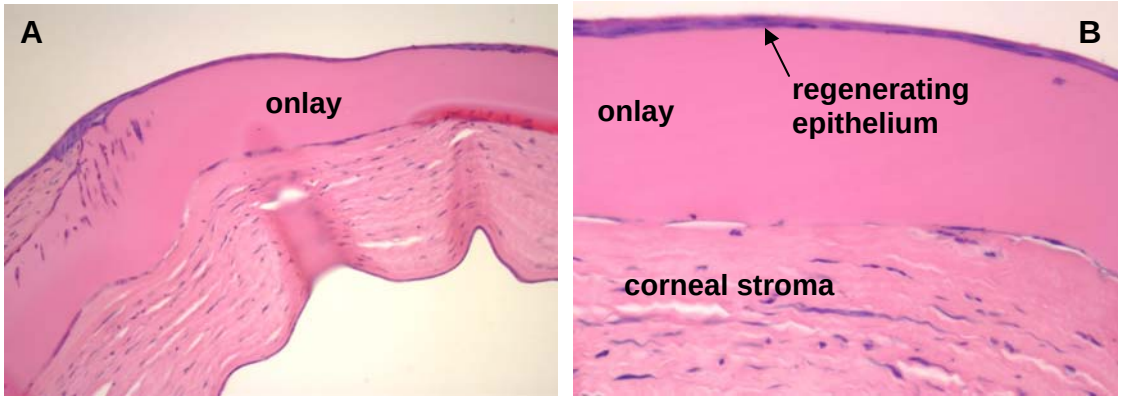

Figure 4.7 Cross-sections of implanted corneal onlays at 7 days post-implantation. Histological sections of low (A) and high (B) magnification are shown; the onlay is 115 μm thick. Epithelium 1-2 layers thick covers the anterior onlay surface. Evidence of the corneal pocket used to hold the onlay can be seen in the left of (A).

4.5 Discussion

The ability of the artificial extracellular matrix protein onlays to support complete re-epithelialization is encouraging, as are the good interface with surrounding tissue and the absence of degradation. The time-course for re-epithelialization, 4-7 days, is faster than the 5-11 days previously reported for collagen I-coated perfluoropolyethers, among the most successful synthetic onlays to date, although the size of the defect here is smaller (3 mm versus 6 mm).[15] The aE-RGD protein films were far more successful in promoting epithelium growth than previously reported synthetic polymer hydrogel lenses coated or tethered with various adhesive peptides and proteins, including fibronectin and RGD; in the best case these required 15 days for randomly seeded rabbit epithelial cells to grow to confluence in culture.[36]

Longer implantation studies using the same implantation technique, for example on a 3-month time scale with periodic sacrifices for evaluation, will be useful in characterizing the patency of the onlays. This time period will give better evidence of onlay degradation and remodeling if it occurs. Electron microscopy can be used to examine the onlay-epithelial interface to establish the presence of adhesion complexes including hemidesmosomes and anchoring fibrils.

To maximize the likelihood of success in these longer studies, the lenses should be sterilized prior to implantation. Because radiation (γ-irradiation) or chemical (ethylene oxide) treatments may change the biochemical or mechanical properties of the aE-RGD protein, heat-based methods such as autoclave

treatment are indicated. Furthermore, extractable bacterial endotoxin should be minimized in future preparations; eliminating the mild immune response to the lenses may simply require more stringent purification techniques to remove this contaminant. Alternatively, two-phase extraction, ion-exchange chromatography, and affinity-based techniques have been used to remove endotoxin from protein solutions.[37]

Depending on the performance of the onlay lenses on longer time scales, it may be necessary to modify the sequence of the aE-RGD protein through recombinant DNA techniques. Easily implemented minor sequence modifications can affect the stiffness[29] or degradation[34] of artificial protein films. The areal density of the RGD cell binding domain on the anterior surface of the onlay may affect epithelial cell adhesion. Alternative cell binding domains might be used to promote adhesion through different integrin receptors.

While artificial proteins or other approaches may solve the issue of epithelial cell adhesion to onlay materials, the significant challenge of devising an optically transparent method to attach the onlay to the anterior surface of the corneal stroma remains. The corneal pocket model is effective for initial evaluation of onlay materials, but the promise of onlays relies on their ability be placed without surgical incisions. Based on histological evaluation, the onlays seem to integrate well into surrounding tissue at 7 days, but a short-term means of securing the onlays is required for the application. Controlled application of tissue adhesives may be a straightforward solution. A photocrosslinking approach, made possible by incorporation of non-canonical amino acids,[38] may

be simpler to implement. The ability to re-engineer the artificial protein sequence may enable still other means of adhesion.

4.6 Conclusions

This preliminary study shows that artificial proteins, designed to mimic key features of the natural extracellular matrix, can be fashioned in the form of contact lenses and successfully implanted into a rabbit cornea. Rabbit corneal epithelial cells adhere to and proliferate over these implanted onlays, which are fairly well tolerated by the rabbit eye despite sterility and contaminant concerns.

Future work in developing the onlay lenses for the application will include more strenuous purification and sterilization procedures. Subsequently, long-term implantation studies will be performed to assess biocompatibility, stability, immune response, and to confirm the ability of the onlays to support mature corneal epithelium. A reliable means of ensuring adhesion between the onlays and the underlying corneal stroma must also be devised.

Acknowledgements.

Keith Duncan aided the surgical implantation studies. Calhoun Vision (Pasadena, CA) is continuing development of the onlays.

4.7 References

(1) Sugar A, Rapuano CJ, Culbertson WW, Huang D, Varley GA, Agapitos PJ, de Luise VP, Koch DD. Laser in situ keratomileusis for myopia and astigmatism: Safety and efficacy - A report by the American Academy of Ophthalmology. *Ophthalmology* **2002**, *109*, 175-187.

(2) Evans MDM, McLean KM, Hughes TC, Sweeney DF. A review of the development of a synthetic corneal onlay for refractive correction. *Biomaterials* **2001**, *22*, 3319-3328.

(3) Lee JB, Seong GJ, Lee JH, Seo KY, Lee YG, Kim EK. Comparison of laser epithelial keratomileusis and photorefractive keratectomy for low to moderate myopia. *J. Cataract Refract. Surg.* **2001**, *27*, 565-570.

(4) Vesaluoma M, Perez-Santonja J, Petroll WM, Linna T, Alio J, Tervo T. Corneal stromal changes induced by myopic LASIK. *Invest. Ophth. Vis. Sci.* **2000**, *41*, 369-376.

(5) Melki SA, Azar DT. LASIK complications: Etiology, management, and prevention. *Surv. Ophthalmol.* **2001**, *46*, 95-116.

(6) Fan-Paul NI, Li J, Miller JS, Florakis GJ. Night vision disturbances after corneal refractive surgery. *Surv. Ophthalmol.* **2002**, *47*, 533-546.

(7) Pushker N, Dada T, Sony P, Ray M, Agarwal T, Vajpayee RB. Microbial keratitis after laser in situ keratomileusis. *J. Refract. Surg.* **2002**, *18*, 280-286.

(8) Lass JH, Stocker EG, Fritz ME, Collie DM. Epikeratoplasty - the surgical correction of aphakia, myopia, and keratoconus. *Ophthalmology* **1987**, *94*, 912-923.

(9) Rao GN, Ganti S, Aquavella JV. Specular microscopy of corneal epithelium after epikeratophakia. *Am. J. Ophthalmol.* **1987**, *103*, 392-396.

(10) Rodrigues M, Nirankari V, Rajagopalan S, Jones K, Funderburgh J. Clinical and histopathologic changes in the host cornea after epikeratoplasty for keratoconus. *Am. J. Ophthalmol.* **1992**, *114*, 161-170.

(11) Thompson KP, Hanna KD, Gipson IK, Gravagna P, Waring GO, Johnsonwint B. Synthetic epikeratoplasty in rhesus-monkeys with human type-IV collagen. *Cornea* **1993**, *12*, 35-45.

(12) Xie RZ, Stretton S, Sweeney DF. Artificial cornea: Towards a synthetic onlay for correction of refractive error. *Biosci. Rep.* **2001**, *21*, 513-536.

(13) Hicks CR, Fitton JH, Chirila TV, Crawford GJ, Constable IJ. Keratoprostheses: Advancing toward a true artificial cornea. *Surv. Ophthalmol.* **1997**, *42*, 175-189.

(14) Latkany R, Tsuk A, Sheu MS, Loh IH, TrinkausRandall V. Plasma surface modification of artificial corneas for optimal epithelialization. *J. Biomed. Mater. Res.* **1997**, *36*, 29-37.

(15) Evans MDM, Xie RZ, Fabbri M, Bojarski B, Chaouk H, Wilkie JS, McLean KM, Cheng HY, Vannas A, Sweeney DF. Progress in the development of a synthetic corneal onlay. *Invest. Ophth. Vis. Sci.* **2002**, *43*, 3196-3201.

(16) Thompson KP, Hanna K, Waring GO, Gipson I, Liu Y, Gailitis RP, Johnson-Wint B, Green K. Current status of synthetic epikeratoplasty. *Refract. Corneal Surg.* **1991**, *7*, 240-248.

(17) Krejchi MT, Atkins EDT, Waddon AJ, Fournier MJ, Mason TL, Tirrell DA. Chemical sequence control of beta-sheet assembly in macromolecular crystals of periodic polypeptides. *Science* **1994**, *265*, 1427-1432.

(18) Petka WA, Harden JL, McGrath KP, Wirtz D, Tirrell DA. Reversible hydrogels from self-assembling artificial proteins. *Science* **1998**, *281*, 389-392.

(19) Ratner BD, Bryant SJ. Biomaterials: Where we have been and where we are going. *Annu. Rev. Biomed. Eng.* **2004**, *6*, 41-75.

(20) Panitch A, Yamaoka T, Fournier MJ, Mason TL, Tirrell DA. Design and biosynthesis of elastin-like artificial extracellular matrix proteins containing periodically spaced fibronectin CS5 domains. *Macromolecules* **1999**, *32*, 1701-1703.

(21) Liu CY, Apuzzo MLJ, Tirrell DA. Engineering of the extracellular matrix: Working toward neural stem cell programming and neurorestoration - Concept and progress report. *Neurosurgery* **2003**, *52*, 1154-1165.

(22) Welsh ER, Tirrell DA. Engineering the extracellular matrix: A novel approach to polymeric biomaterials. I. Control of the physical properties of artificial protein matrices designed to support adhesion of vascular endothelial cells. *Biomacromolecules* **2000**, *1*, 23-30.

(23) Liu JC, Heilshorn SC, Tirrell DA. Comparative cell response to artificial extracellular matrix proteins containing the RGD and CS5 cell-binding domains. *Biomacromolecules* **2004**, *5*, 497-504.

(24) Ruoslahti E. RGD and other recognition sequences for integrins. *Annu. Rev. Cell Dev. Biol.* **1996**, *12*, 697-715.

(25) Urry DW, Parker TM, Reid MC, Gowda DC. Biocompatibility of the bioelastic materials, poly(GVGVP) and its gamma-irradiation cross-linked matrix - summary of generic biological test-results. *J. Bioactive and Compatible Polym.* **1991**, *6*, 263-282.

(26) Chapman HA, Riese RJ, Shi GP. Emerging roles for cysteine proteases in human biology. *Annu. Rev. Physiol.* **1997**, *59*, 63-88.

(27) Torchia DA, Piez KA. Mobility of elastin chains as determined by C-13 nuclear magnetic resonance. *J. Mol. Biol.* **1973**, *76*, 419-424.

(28) Li B, Alonso DOV, Daggett V. The molecular basis for the inverse temperature transition of elastin. *J. Mol. Biol.* **2001**, *305*, 581-592.

(29) Di Zio K, Tirrell DA. Mechanical properties of artificial protein matrices engineered for control of cell and tissue behavior. *Macromolecules* **2003**, *36*, 1553-1558.

(30) Evans MDM, Xie RZ, Fabbri M, Madigan MC, Chaouk H, Beumer GJ, Meijs GF, Griesser HJ, Steele JG, Sweeney DF. Epithelialization of a synthetic polymer in the feline cornea: A preliminary study. *Invest. Ophth. Vis. Sci.* **2000**, *41*, 1674-1680.

(31) Urry DW. Physical chemistry of biological free energy transduction as demonstrated by elastic protein-based polymers. *J. Phys. Chem. B* **1997**, *101*, 11007-11028.

(32) Nowatzki PJ, Tirrell DA. Physical properties of artificial extracellular matrix protein films prepared by isocyanate crosslinking. *Biomaterials* **2004**, *25*, 1261-1267.

(33) Lee J, Macosko CW, Urry DW. Swelling behavior of gamma-irradiation cross-linked elastomeric polypentapeptide-based hydrogels. *Macromolecules* **2001**, *34*, 4114-4123.

(34) (Chapter 3) Heilshorn SC, Nowatzki PJ, Yamaoka T, Tirrell DA. Controlled proteolytic degradation of protein-based biomaterials. *Prepared for submission.*

(35) Nagapudi K, Brinkman WT, Leisen J, Thomas BS, Wright ER, Haller C, Wu XY, Apkarian RP, Conticello VP, Chaikof EL. Protein-based thermoplastic elastomers. *Macromolecules* **2005**, *38*, 345-354.

(36) Jacob JT, Rochefort JR, Bi JJ, Gebhardt BM. Corneal epithelial cell growth over tethered-protein/peptide surface-modified hydrogels. *J. Biomed. Mater. Res. B* **2005**, *72B*, 198-205.

(37) Petsch D, Anspach FB. Endotoxin removal from protein solutions. *J. Biotechnol.* **2000**, *76*, 97-119.

(38) (Appendix) Carrico IS, Heilshorn SC, Mock ML, Liu JC, Nowatzki PJ, Maskarinec SA, Franck C, Ravichandran G, Tirrell DA. Lithographic patterning of intrinsically photoreactive cell-adhesive proteins. *Prepared for submission.*